Magnetoresistance in granular magnetic tunnel junctions with Fe nanoparticles embedded in ZnSe semiconducting epilayer

A. R. de Moraes, C. K. Saul, D. H. Mosca, J. Varalda, P. Schio et al.

Magnetoresistance in granular magnetic tunnel junctions with Fe nanoparticles embedded in ZnSe semiconducting epilayer

A. R. de Moraes,[1,a)] C. K. Saul,[1] D. H. Mosca,[1] J. Varalda,[2] P. Schio,[2] A. J. A. de Oliveira,[2] M. A. Canesqui,[3] V. Garcia,[4] D. Demaille,[4] M. Eddrief,[4] V. H. Etgens,[4] and J. M. George[5,6]

[1]*Departamento de Física, Universidade Federal do Paraná, C. P. 19091 81531-990 Curitiba PR, Brazil*
[2]*Departamento de Física, Universidade Federal de São Carlos, C. P. 676, 13565-905 São Carlos SP, Brazil*
[3]*Centro de Componentes Semicondutores, Universidade Estadual de Campinas, 13083-870 Campinas, SP Brazil*
[4]*Institut des NanoSciences de Paris, Universités Paris 6 et Paris 7, CNRS UMR 7588, 140 rue de Lourmel, 75015 Paris, France*
[5]*Unité Mixte de Physique CNRS-Thales, Route départementale 128, 91767 Palaiseau Cedex, France*
[6]*Université Paris-Sud 91405, Orsay, France*

We have investigated transport properties of iron (Fe) nanoparticles embedded in zinc selenide (ZnSe) semiconducting epilayers prepared by molecular beam epitaxy. Both positive and negative tunneling magnetoresistances (TMRs) were measured depending on the applied voltage biases and on the temperature. A slow reduction of the TMR magnitude with temperature was detected and it could be explained in terms of a crossover between direct/resonant tunneling and variable range hopping. The temperature behavior of the magnetoresistance is a clear signature of tunneling and hopping mechanisms mediated by the ZnSe barrier localized states. © *2008 American Institute of Physics*. [DOI: 10.1063/1.2938071]

I. INTRODUCTION

The integration of ferromagnetic and semiconductive materials in a room-temperature functional device is a major step toward the spintronic technology.[1] One realistic way to investigate and test different materials is through the study of transport properties on magnetic tunnel junctions (MTJs) formed by two ferromagnetic electrodes separated by a semiconductive barrier layer. When electrically polarized, the carriers can tunnel through the barrier from electrode to the other. *A priori*, the relative orientations of the magnetizations are controlled by an external magnetic field and the difference between the states of resistance from parallel to antiparallel magnetization configurations determine the magnitude of tunnel magnetoresistance (TMR) effect. Simultaneously, the impetus to investigate assemblies of interacting and non-interacting magnetic nanoparticles embedded in a solid matrix is pushed by the increasing miniaturization of electronic devices for applications in ultrahigh-density magnetic recording and spin-based on/off switching devices.[2] In magnetic granular systems, the carrier tunneling between magnetic particles could increase the Coulomb energy by a charging effect. This effect, known as Coulomb blockade,[3] could promote novel phenomena.[4–8]

In this work, we report on the magnetotransport measurements of granular MTJ systems, formed by an ensemble of Fe nanoparticles embedded in a ZnSe epilayer grown by molecular beam epitaxy. We have studied, transport properties using both sample plane perpendicular current (CPP) geometry and in plane current geometry in Fe–ZnSe granular

samples, prepared by using the same fabrication procedure.[9] Previous studies have already attested the potential of Fe/ZnSe heterostructures for spin polarized injection and detection studies,[10] due to the favorable lattice matching, stable interfacial magnetism,[11] and nearly ideal Schottky barrier formation.[12] Besides, it has been demonstrated that the spin coherent transport can be successfully achieved in ZnSe at room temperature for time intervals close to microsecond, which corresponds to typical distances required for applications in microeletronics.[13]

II. EXPERIMENTAL PROCEDURE

The samples were grown by a molecular beam epitaxy growth facility with separate III-V and II-IV growth chambers. A 10-nm-thick ZnSe strained epilayer was grown on a 100-nm-thick GaAs buffer layer grown on commercial GaAs(001) substrate with standard growth conditions.[14] Iron was supplied by a Knudsen cell on the II-VI growth chamber with a rate of ~ 0.2 nm/min. The base pressure during deposition was below 5×10^{-10} mbar. As previously reported, the very beginning of Fe nucleation on the (001) ZnSe surface proceeds by the formation of isolated islands[9,15] up to a 0.4 nm nominal thickness, when coalescence starts. A crystalline assembly of Fe nanoparticles epitaxied on ZnSe surface can be obtained by stopping the growth below this percolation limit. The next step was to separate the successive planes of Fe clusters by covering them with a 4.5-nm-thick crystalline ZnSe epilayer. The whole structure was grown at 200 °C in order to both promote a good crystalline quality of ZnSe epilayers and to limit eventual interdiffusion between Fe and ZnSe.[16] This procedure surprisingly produces metal-
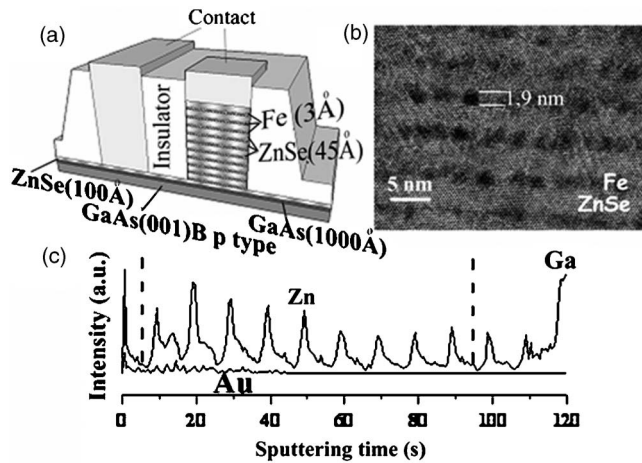
FIG. 1. (a) Schematic diagram showing the MTJ microfabricated by optical lithography. (b) Cross-sectional TEM image showing Fe nanoparticles (dark regions) embedded in the ZnSe epilayer (grey region) onto ZnSe/GaAs substrate. (c) SIMS profile illustrating the chemical modulation of Zn, which attests the integrity of the ZnSe spacer layers.
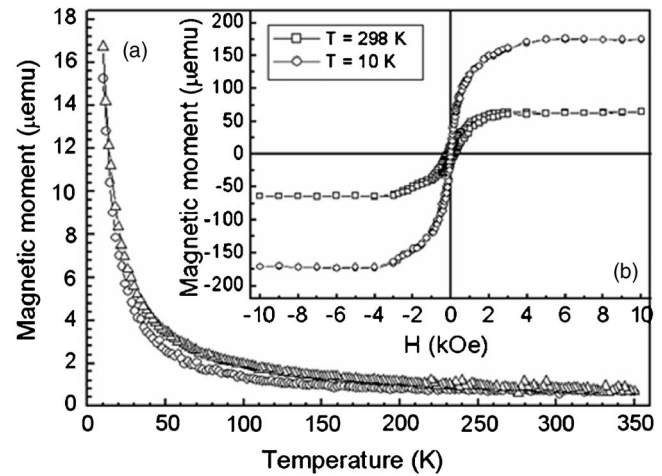

FIG. 2. (a) ZFC (open circles) and FC (up triangles) magnetic moment curves measured with magnetic field of 50 Oe. (b) Hysteresis cycles measured at 10 and 298 K. Both experiments were performed with the magnetic field applied in the film plane.

lic Fe nanoparticles embedded in ZnSe with a uniform distribution of size, shape and interspacing distances. A "multilayer" was obtained by repeating by ten times this procedure. At the end, the samples were covered by a protective Au layer.

The transport experiments here described were performed in CPP geometry, using MTJs prepared by optical lithography with pillar structures having areas of 8 and 64 μm^2. A schematic diagram of the microfabricated MTJ with pillar geometry is shown in Figure 1(a). Cross-sectional transmission electron microscopy (FEM) images [Fig. 1(b)] and secondary ion mass spectroscopy (SIMS) profile [Fig. 1(c)] reveal a chemical modulation with ten Zn-richer layers of heterostructure. The ZnSe layer is continuous and no physical contacts were observed between the planar assemblies of almost monodisperse iron nanoparticles. The particle volume estimated from magnetic measurements are compatible with the size estimation obtained by TEM micrograph. SIMS profile was used to accurately place the electrical contacts in the bottom clusters plane for CPP geometry of measurements, as indicated in Fig. 1(a).

III. MAGNETIC CHARACTERIZATION

The magnetic measurements were performed with a superconducting quantum interference device magnetometer (Quantum Design MPMS-5S). Zero-field cooling (ZFC) and field cooling (FC) routines were used in magnetization as a function of temperature measurements, as shown in Fig. 2(a). No peak is observable in the ZFC curve indicating that even at 10 K, the sample is not magnetically blocked. A small irreversibility between ZFC and FC curves is observed for a cooling field of 50 Oe. Figure 2(b) shows the magnetic moment versus applied field curves $M(H)$ measured at 10 and 298 K. These hysteresis loops present moderate coercive fields ($H_C < 25$ Oe at 10 K and $H_C \sim 200$ Oe at 298 K) and remanence ($M_R \sim 3\%$ M_S at 10 K and $M_R \sim 25\%$ M_S at 298 K) with respect to the saturation magnetization M_S. The increase in the hysteretic behavior observed at 298 K can be

related to the frustration effects, caused by thermally activated exchange coupling, already described in the literature for a Fe/ZnSe/Fe trilayer.[17] Langevin fittings of the $M(H)$ curve at 10 K lead to a mean magnetic moment per particle of 600 bohrs magnetons (μ_B). We estimate that the mean magnetic volume is $V = 600\mu_B/M_S \sim 3.25$ nm^3, where $M_S = 1710$ emu/cm^3 is the saturation magnetization of Fe. This result leads to a superparamagnetic blocking temperature $T_B = VK_{Fe}/25k_B \sim 4.2$ K, taking k_B as the Boltzmann constant and $K_{Fe} = 4.5 \times 10^6$ erg/cm^3, as previously observed.[15] This T_B value is below the measured range and it also explains why a significant magnetic irreversibility is not observed in the ZFC-FC curves.

IV. MAGNETOTRANSPORT MEASUREMENTS

All the electric measurements were performed over the range of 2–298 K, using a Physical Properties Measurement System (Quantum Design) system with an external source meter to apply voltage biases from +7 to −7 V. The maximum magnitude of the applied bias was kept at 7 V to avoid dielectric breakdown of the MTJs. Despite the scrupulous reproduction of the microfabrication procedures, the room-temperature surface resistance (ratio between resistance and junction cross-sectional area) varies from 3 MΩ to 13 kΩ for junctions with areas ranging from 8 to 128 μm^2 for two granular samples prepared under similar growth conditions. We describe magnetoresistance found in the smallest MTJs with areas of 8 and 64 μm^2.

Figure 3(a) shows the temperature dependence of the resistance, attesting a semiconductor behavior and an almost temperature-independent tunneling regime at low temperatures. For the complete set of microfabricated MTJs, the temperature dependence of the surface resistance always presents a similar semiconducting behavior. Nonlinear and asymmetric behavior of the conductance versus bias curves were observed for temperatures between 2 and 298 K, as shown in Fig. 3(b), for a junction with area of 64 μm^2. This
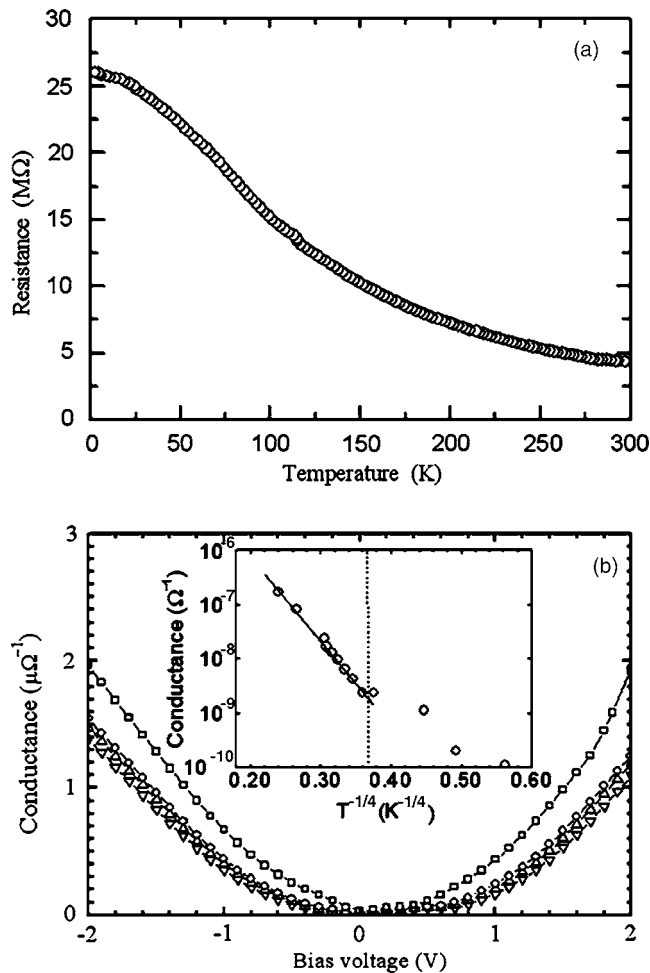
FIG. 3. (a) Resistance of the 8 μm^2 area junction as a function of the temperature, under voltage bias of U=1.5 V. An almost temperature-independent tunnel regime is observed at low temperature. (b) Conductance versus bias for a 64 μm^2 area junction at four temperatures: ($\square$) 90 K, ($\bigcirc$) 60 K, ($\triangle$) 25 K, and ($\triangledown$) 5 K. Nonlinear and asymmetric effects are quite noticeable even at low bias. The inset shows the conductance versus temperature for this junction. For temperatures above 50 K, the conductance is well described by the variable range hopping theory. The solid line is the best fitting using 1/4 for power exponent value.

asymmetry of the conductance versus bias suggests a non-uniform distribution of defects in the ZnSe matrix from bottom to top electrodes of the MTJ.

These results can be used to capture the essential physics of the conductance in the presence of localized states within the ZnSe matrix, which is either dominated by direct and resonant tunneling or inelastic hopping, through chains of two or more localized states. It is expected that the conductance at low bias consists of a bias-independent term, which includes temperature-independent direct and resonant tunneling contributions, and a voltage bias/temperature-dependent term associated with the onset of hopping processes.[18] The inset of Fig. 3(b) shows a semilogarithmic scale plot of the conductance versus $T^{-1/4}$ for the junction with the area of 64 μm^2. The conductance behavior at temperatures higher than 50 K follows closely the prediction of variable range hopping theory.[18] Junctions with 8 and 64 μm^2 give best fitting for the $T^{-1/4}$ law in the same temperature region. One may question the objectiveness of this procedure, where the

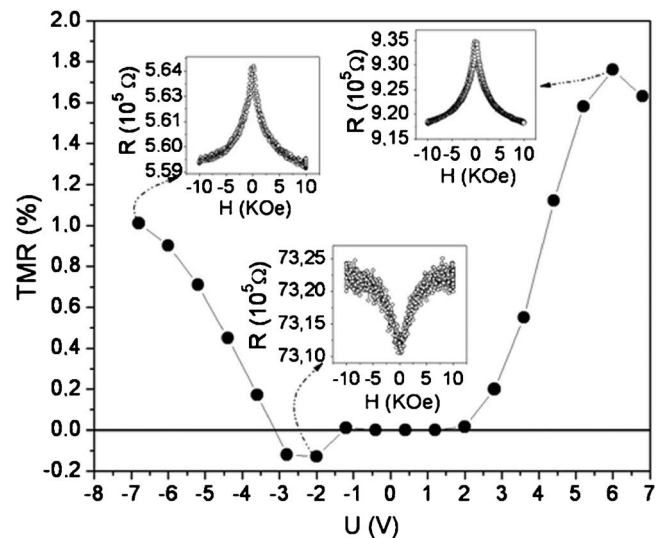FIG. 4. Tunneling magnetoresistance vs voltage bias, as measured at 10 K for 8 μm^2 junction. The three insets show the resistance vs magnetic fields for representative voltage biases U=−7, −3, and +6 V.

power law is sensitive to temperature range chosen for the fitting. However, we are just testing the power exponent suitability to prove beyond reasonable doubt, that the nonlinear conductance at these temperatures can be related to hopping processes, involving almost uniform distribution of localized states. We conclude that both tunnel and hopping conductions are present, leading to a purely statistical configuration of conduction channels (in energy and space) as a function of the temperature, voltage, and distance between nanoparticles. As temperature and voltage increase, the dominant contribution to the conduction comes from channels with larger and larger numbers of localized states.

Figure 4 presents the TMR obtained from the $R(H)$ curves by the expression $100\times[R(H) -R(10\ \text{kOe})]/R(10\ \text{kOe})$, revealing an asymmetry behavior with respect to the applied voltage bias U at 10 K. For $U >0$, TMR is negative (resistance is lower at high magnetic field) with magnitude increasing up to U=+6 V, when a slight decrease is observed. For $U<0$, TMR is positive (resistance is higher at high magnetic field) for −3 V$<U<$ −1 V and once again becomes negative for $U<$−3 V. The insets show $R(H)$ curves for three representative values of voltage bias U. When TMR is negative, the resistance maxima are observed at field of about 250 Oe, whereas the $M(H)$ curve in 10 K presents $H_C<$ 25 Oe. When TMR is positive, the resistance minima occur at fields of 175 Oe. Therefore, the maxima and minima of resistance are not correlated with the H_C values at low temperatures.

Figure 5(a) shows the $R(H)$ curves measured at room temperature for U=+3 and −3 V. The resistance values and TMR magnitudes are distinct for these two symmetric voltages without evidence of saturation for magnetic fields up to 30 kOe. Indeed, the magnetization is already saturated at 5 kOe. The thermal evolution of TMR for different biases U is shown in Fig. 5(b). For $U>0$, TMR magnitude decreases for increasing temperature. The TMR signal reverses at 115 K for U=−2 V. For U=−4 V, the TMR magnitude remains almost temperature independent. Therefore, the signal
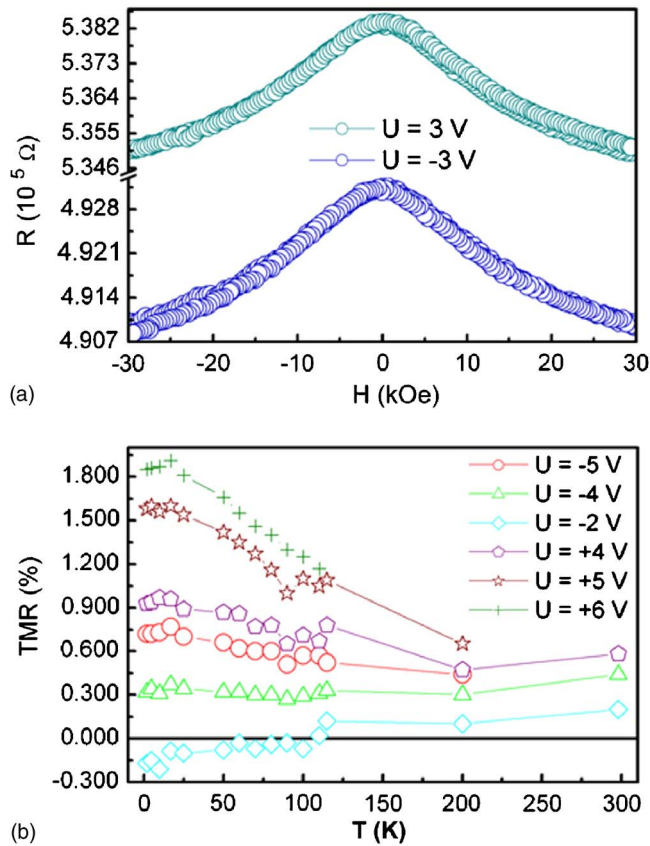
FIG. 5. (Color online) (a) Resistance vs magnetic field measured at room temperature with symmetric opposite voltage biases. (b) Thermal evolution of the tunneling magnetoresistance for some voltage biases. Measurements were performed in a 64 μm^2 junction.

of TMR reverses as a function of voltage bias at a fixed temperature (Fig. 4), when tunneling conductance is predominant, and as a function of temperature at a fixed voltage bias, as shown in Fig. 5(b), when hopping processes are present.

V. DISCUSSION

In the present samples, two issues contribute mainly to enhance the formation of defects in the ZnSe epilayers. First, the growth of a semiconducting epilayer on top of a cluster assembly of a dissymmetric material such as iron. Second, the undoped ZnSe layers were grown at low temperature to avoid interdiffusion effects, enhancing the probability to introduce defects such as Zn antisites and eventually dislocations. These kinds of defects (also Fe dopant can be formed)[19] in ZnSe originate a midgap band (~ 0.2 eV) of donor deep levels and *n*-type undoped ZnSe that is mainly formed as a consequence of compensation mechanisms.[20–22] Conductance dominated by resonant tunneling of electrons mediated by localized midgap states in the ZnSe barrier has already been observed by our group for planar Fe/ZnSe/Fe tunnel junctions.[20] These defect states present energies (E_d) lying near the Fermi energy (E_F), which in the case of Fe/ZnSe junction, is located around the center of the energy band gap ($E_G \sim 2.7$ eV) of ZnSe. When the energy introduced by the voltage bias (eU), together with the thermal energy ($k_B T$), satisfies the condition $E_F + k_B T + eU \sim E_d$, reso-

nant tunneling occurs. For symmetric positions of defect states, the TMR signal is maintained as designed by the electrodes spin polarizations. The TMR signal is mainly inversed due to the asymmetric positions of defects inside the ZnSe barriers, which determines distinct leak rates from injector to detector centers. This mechanism can induce TMR inversion as firstly described by Tsymbal *et al.*[23] in Ni/NiO/Co nanojunctions. Both signal inversion and small amplitude of TMR suggest a large and nonuniform distribution of defects in the ZnSe.[20] In fact, we expect that structural defects are cumulative, increasing from bottom to top in the MTJ structure.

The interpretation of magnetoresistance in our granular MTJs is much more demanding compared to a MTJ with a simple tunnel barrier. Peralta-Ramos and Llois[24] have recently studied Fe/ZnSe/Fe/ZnSe/Fe double MTJs by *ab initio* calculation at zero temperature. They have found that the TMR in these double junctions should be higher than for a simple MTJ. The TMR enhancement was mainly related to a drop in the conductance of some spin channels due to the spin-filter effect in a direct tunneling regime, being practically independent of the in-between Fe layer thickness.

Our granular MTJs present a weak variation of the resistance below 50 K, as observed in Fig. 3(a) and nonlinear and asymmetric conductance versus bias, as shown in Fig. 3(b). It indicates that the direct tunneling may represent an important contribution to the total conductance. However, the observed inversion of TMR signal also indicates a conductance in the resonant tunneling regime mediated by midgap localized states. Thus, we assume that both direct and resonant tunneling conductances are concurrent in our granular MTJs. The small TMR values measured for our samples at low temperature can be related to the strong decrease of the direct tunneling conductance, as previously described, for the observed TMR enhancement in double MTJs,[24] and due to resonant conductance averaging over the defect states in the ZnSe barrier.[20–27]

The $R(H)$ curves shown in the insets of Fig. 4 illustrate that the resistance changes $-\Delta R$ are small compared to junction resistances. The TMR increase with voltage bias U is mainly due to the resistance drop with applied voltage bias either positive or negative. According to previous works, it is not surprising that the presence of defects and impurities in the MTJs may strongly reduce or even suppress the TMR.[23,24,26] However, the small and bias-reversible TMR found at low temperatures is most likely caused by the tunnel conductance averaged over the resonant states.[23] In the ideal case of a MTJ with Fe electrodes and symmetrical position of defect states in the barrier, the conductance averaging leads to a maximum TMR of 4%.[25] It is expected that assimetrical positions of defect states in the barrier can diminish even more the TMR.[18,21]

For increasing temperature, the conductance, essentially described by the direct and resonant tunneling contributions, must include a temperature-dependent term to account for the onset of hopping processes. Hopping distances as large as 4.2–5.8 nm are reported in the nanocrystalline ZnSe films.[27] Variable range hopping between Fe nanoparticles is plausible due to the interparticle spacing of about 4.5 nm. However, the midgap defect states are quite closed to the Fermi level,

as evidenced by the observed resonant tunneling, favoring the hopping through ZnSe. The crossover from direct and resonant tunneling to predominantly variable range hopping is accompanied by a striking result, in which the TMR magnitude drops slowly as the temperature rises up to 298 K. The hopping conductance over multiple channels with more localized states is expected to become progressively important, resulting in increasingly nonlinear conductances, as shown in Fig. 3(b). The TMR magnitude decreases for increasing temperature whatever bias applied, as shown in Fig. 5(b), because ΔR diminishes faster than R for increasing temperature. Notably, a small spin-dependent conductance persists in the predominantly hopping regime and the inverse magnetoresistance becomes normal above 110 K for $U=-2$ V. Thus, the crossover from resonant tunneling to variable range tunneling regime decreases the magnetoresistance and even change its signal.

Let us finally address the noncoincidence of resistance maxima or minima with coercive fields at low temperatures, and the absence of saturation effects in the TMR curves, for magnetic fields much higher than the fields necessary to saturate the magnetization of the samples as shown, for example, in Fig. 5(b). One possible explanation is that thermally activated exchange coupling, as described in Ref. 17, can be intervene in the magnetic moment configuration. Indeed, Zhuravlev *et al.*[28] have demonstrated that antiferromagnetic coupling strength, averaged over randomly distributed impurity or defect positions inside tunnel barriers, exhibits a monotonic increase with temperature when the energy of impurity or defect states matches the Fermi energy. We have already observed experimentally the linear increase of the antiferromagnetic exchange coupling in planar Fe/ZnSe/Fe structures.[17] A weak exchange coupling with resonant character is physically reasonable between Fe nanoparticles embedded in ZnSe and is consistent with our experimental observations in the magnetization cycles and also with our previous work on such kind of structures.[9] However, another possibility to explain the noncoincidence of these fields could involve the assumption of a strong enough current density, capable to induce a torque transfer to a ferromagnetic nanoparticle in the Coulomb blockaded regime, changing its magnetic moment orientation. The mean volume of the Fe particles (spheroidal shape with diameter of ~ 1.9 nm) is small enough to imply that most of particles are Coulomb blocked even at room temperature. The Coulomb blockade energy[29,30] calculated by $E_C=(e^2/2\pi\varepsilon_0\varepsilon d)/(1+d/2s)$ is estimated as 140 meV, which is a value higher than the thermal energy at 298 K. In this equation, e is the electron charge, ε_0 is the permittivity of space, $\varepsilon=9.2$ is the ZnSe dielectric constant,[31] $d\sim 1.9$ nm is the particle diameter, and $s=4.5$ nm is the mean interparticle distance (ZnSe spacer layer). A similar observation of the noncoincidence of resistance maxima or minima with coercive fields at low temperatures is reported in Co nanoparticles embedded in TiO_2 matrix.[32] New experiments are needed to clarify the mechanisms of the observed phenomena.[33]

VI. SUMMARY AND CONCLUSION

We have studied the transport in epitaxial granular MTJ. The results are interpreted in terms of an underlying tunnel and hopping conduction via localized states created by defect sites or traps. These results clarify both the consequences of the presence of localized states in the ZnSe barrier spacers and the nature of transport in disordered semiconductor at nanometer length scale. The correlation between tunnel and hopping processes discussed here is not completely understood, however, it may be of fundamental interest. Finally, we point out that the effects of localized states on magnetoresistance of semiconducting systems for increasing temperature result in a crossover from a TMR to an all-metallic-magnetoresistance (called giant-magnetoresistance) mechanism, which is not yet well understood. The potential of the granular systems within a semiconductor host, studied here, has not been explored and may be useful in the design of future metal-semiconductor spintronic devices.

[1]S. A. Wolf, D. D. Awschalom, R. A. Buhrman, J. M. Daughton, S. von Molnár, M. L. Roukes, A. Y. Chtchelkanova, and D. M. Treger, Science **294**, 1488 (2001).
[2]R. H. Kodama, J. Magn. Magn. Mater. **200**, 359 (1999).
[3]B. Abeles, Ping Sheng, M. D. Coutts, and Y. Arie, Adv. Phys. **24**, 407 (1975).
[4]D. L. Peng, K. Sumyiama, T. J. Konno, T. Hihara, and S. Yamamuro, Phys. Rev. B **60**, 2093 (1999).
[5]L. F. Schelp, A. Fert, F. Fettar, P. Holody, S. F. Lee, J. L. Maurice, F. Petroff, and A. Vaurès, Phys. Rev. B **56**, R5747 (1997).
[6]H. Zare-Kolsaraki and H. Micklitz, Phys. Rev. B **67**, 224427 (2003).
[7]K. Yakushiji, S. Mitani, F. Ernult, K. Takanashi, and H. Fujimori, Phys. Rep. **451**, 1 (2007).
[8]P. Seneor, A. Bernand-Mantel, and F. Petroff, J. Phys.: Condens. Matter **19**, 165222 (2007).
[9]J. Varalda, G. A. P. Ribeiro, M. Eddrief, M. Marangolo, J. M. George, V. H. Etgens, D. H. Mosca, and A. J. A. de Oliveira, J. Phys. D **40**, 2421 (2007).
[10]X. Jiang, A. F. Panchula, and S. S. P. Parkin, Appl. Phys. Lett. **83**, 5244 (2003).
[11]M. Marangolo, F. Gustavsson, M. Eddrief, Ph. Sainctavit, V. H. Etgens, V. Cros, F. Petroff, J. M. George, P. Bencok, and N. M. Brooks, Phys. Rev. Lett. **88**, 217202 (2002).
[12]M. Eddrief, M. Marangolo, S. Corlevi, G. M. Guichar, V. H. Etgens, R. Mattana, D. H. Mosca, and F. Sirotti, Appl. Phys. Lett. **84**, 4553 (2002).
[13]I. Malajovich, J. J. Berry, N. Samarth, and D. D. Awschalom, Nature (London) **411**, 770 (2001).
[14]V. H. Etgens, B. Capelle, L. Carbonell, and M. Eddrief, Appl. Phys. Lett. **75**, 2108 (1999).
[15]M. Marangolo, F. Gustavsson, G. M. Guichar, M. Eddrief, J. Varalda, V. H. Etgens, M. Rivoire, F. Gendron, H. Magnan, D. H. Mosca, and J. M. George, Phys. Rev. B **70**, 134404 (2004).
[16]D. H. Mosca, M. Abbate, W. H. Schreiner, V. H. Etgens, and M. Eddrief, J. Appl. Phys. **90**, 5973 (2001).
[17]J. Varalda, J. Milano, A. J. A. de Oliveira, E. M. Kakuno, I. Mazzaro, D. H. Mosca, L. B. Steren, M. Eddrief, M. Marangolo, D. Demaille, and V. H. Etgens, J. Phys.: Condens. Matter **19**, 9105 (2006).
[18]Y. Xu, D. Ephron, and M. R. Beasley, Phys. Rev. B **52**, 2843 (1995).
[19]M. Suma, M. Golewski, and T. P. Surkova, Phys. Rev. B **50**, 8319 (1994).
[20]J. Varalda, A. J. A. de Oliveira, D. H. Mosca, J. M. George, M. Eddrief, M. Marangolo, and V. H. Etgens, Phys. Rev. B **72**, 081302(R) (2005).
[21]D. H. Mosca, J. M. George, J. L. Maurrice, A. Fert, M. Eddrief, and V. H. Etgens, J. Magn. Magn. Mater. **226**, 917 (2001).

[22]P. K. Lim and D. E. Brodie, Can. J. Phys. **55**, 1641 (1977).

[23]E. Y. Tsymbal, A. Sokolov, I. F. Sabirianov, and B. Doudin, Phys. Rev. Lett. **90**, 186602 (2003).

[24]J. Peralta-Ramos and A. M. Llois, Phys. Rev. B **73**, 214422 (2006).

[25]A. M. Bratkovsky, Phys. Rev. B **56**, 2344 (1997).

[26]R. Stratton, J. Phys. Chem. Solids **23**, 1177 (1962).

[27]S. K. Mandal, S. Chaudhuri, and A. K. Pal, Nanostruct. Mater. **10**, 607 (1998).

[28]M. Ye. Zhuravlev, E. Y. Tsymbal, and A. V. Vedyayev, Phys. Rev. Lett. **94**, 026806 (2005).

[29]J. Varalda, B. Vodungbo, W. A. Ortiz, A. J. A. de Oliveira, Y.-L. Zheng, D. Demaille, M. Marangolo, and D. H. Mosca, J. Appl. Phys. **100**, 014318 (2006).

[30]S. Mitani, H. Fujimori, and K. Takanashi, J. Magn. Magn. Mater. **198–199**, 179 (1999).

[31]I. Strzalkowski, S. Joshi, and C. R. Crowell, Appl. Phys. Lett. **28**, 350 (1976).

[32]J. Varalda, W. A. Ortiz, A. J. A. de Oliveira, B. Vodungbo, Y. Zheng, D. Demaille, M. Marangolo, and D. H. Mosca, J. Appl. Phys. **101**, 014318 (2007).

[33]J. Slonczewski, J. Magn. Magn. Mater. **159**, L1 (1996).